Monatshefte für Chemie - Chemical Monthly (2023) 154:585–594
https://doi.org/10.1007/s00706-023-03071-6

ORIGINAL PAPER

# The electrostatic immobilization of the horseradish peroxidase on poly-L-histidine modified multiwall carbon nanotube—ionic liquid composite glassy carbon electrode for the amperometric determination of hydrogen peroxide

**Elif Ulukan**[1] · **Funda Öztürk**[1]

Received: 18 February 2023 / Accepted: 20 April 2023 / Published online: 3 May 2023


## Abstract

In this study, an amperometric biosensor for hydrogen peroxide quantification was prepared by electrostatic immobilization of horseradish peroxidase on a multi-walled carbon nanotube, ionic liquid, and poly-L-histidine modified glassy carbon electrode. The immobilization of the horseradish peroxidase on the electrode surface was achieved by positive charges of poly-L-histidine. The surface morphology was analyzed by scanning electron microscopy, cyclic voltammetry, and impedance spectroscopy. The electrode composition, buffer pH, and operating potential were all optimized in order to achieve the best analytical performance. The modified electrode, which has been fabricated at its optimum composition, reveals two different linear working ranges, namely $2.0\times10^{-8}$ M to $9.1\times10^{-7}$ M and $1.8\times10^{-6}$ M to $1.8\times10^{-4}$ M, which are at the determined optimum operating conditions. The detection limit of the proposed method is of $2.9\times10^{-9}$ M. The analytical applicability of the amperometric determination of hydrogen peroxide concerning the developed biosensor has been evaluated by quantifying hydrogen peroxide in a commercial oxygenated water sample.

### Graphical abstract

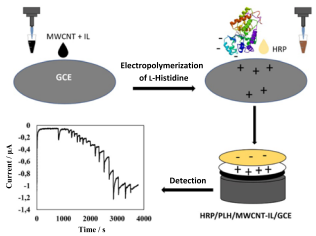


**Keywords** Biosensors · Electrochemistry · Enzymes · Hydrogen peroxide · Poly-L-histidine

## Introduction

Hydrogen peroxide ($H_2O_2$) is a common oxidant currently used in a wide range of industries, such as textile, paper, food, and pharmaceutical ones [1, 2]. In recent years, studies have shown that the excessive use of $H_2O_2$ in food industry is harmful to human health. Consequently, the Food and Agriculture Organization of the United States has limited the highest level of $H_2O_2$ in dairy products to 0.05% (14.7 mM). According to the Joint Expert Committee on Food Additives (JECFA, 2004), the maximum addition of $H_2O_2$ to food must be of 60 mg $kg^{-1}$, whereas the Chinese National Standard (GB5009.226–016) has established this value to be less than 3 mg $kg^{-1}$ [1]. In addition, studies have shown that high levels of $H_2O_2$ in living organisms affect profoundly the natural, physiological processes and can lead to cardiovascular and vascular

✉ Funda Öztürk
fozturk@nku.edu.tr

[1] Department of Chemistry, Faculty of Science and Art, Tekirdağ Namık Kemal University, Tekirdağ, Türkiye

diseases, as well as cancer, neurodegeneration, DNA damage, and so on [3, 4]. The level of $H_2O_2$ in human blood ranges from 1.0 to 5.0 µM, whereas in inflammatory diseases this value can reach up to 50 µM [1]. It is very important to determine the values of $H_2O_2$ in food and clinical diagnostics, particularly because oxidase enzymes also produce $H_2O_2$ as an important intermediate product. The rapid and accurate determination of the $H_2O_2$ is also of great importance in the development of effective biosensors [5]. Various techniques, such as chemiluminescence [6], spectrophotometry [7], titrimetry [8], chromatography [9], and electrochemistry [10–15] have been reported in the literature with regard to the determination of $H_2O_2$. Among these techniques, enzymatic biosensors are more attractive than others since they are inexpensive, simple, sensitive, and selective.

Carbon-based nanomaterials are widely used in biosensor studies due to their ability to provide large surface area, good mechanical and chemical stability, and high electrical conductivity [16]. Biosensors using carbon nanotubes (CNTs) as modification materials have been reported to exhibit high sensitivity, low detection limits, and wide working ranges [17, 18]. In biosensor fabrication, CNTs have been used with ionic liquids (ILs) to obtain composites with high sensitivity and good biocompatibility [19].

ILs belong to a special group of ionic electrolytes without molecular solvents [20]. ILs are used to improve the response of electrochemical biosensors due to their high ionic conductivity and biocompatibility [21]. Moreover, they are chemically and thermally stable as well as relatively ion-conductive, and display negligible vapor pressure, while possessing a wide electrochemical potential range [12]. Imidazolium and pyridinium salts are the main classes of ILs. They have attracted a significant degree of interest. The use of imidazolium ILs as physical films [20, 22–25] or in combination with carbon paste as bulk modified electrodes [26–28] is a major advancement in the field of electrochemistry.

Horseradish peroxidase (HRP) is a monomeric heme-containing phytoenzyme, which has attracted great interest in biosensor and biotechnology applications due to its high stability in the aqueous solution [29]. HRP contains a prosthetic heme group which catalyzes the oxidation of different substrates [5]. The enzymatic activity of HRP is due to the oxidation and reduction of the iron atom in the heme group. The immobilization step in enzyme-based biosensor fabrication determines the reliability and performance of the biosensor. Conventional immobilization methods include non-covalent (entrapment and adsorption) or covalent immobilization [30]. Each of these methods has both advantages and disadvantages. Various enzyme-based electrochemical biosensors have been reported as being used for $H_2O_2$ determination [13–15], but such studies involve complex enzyme immobilization procedures.

Poly-L-histidine (PLH) is a synthetic polyamino acid containing an imidazole group. PLH can be used to facilitate both the reduction and oxidation of myoglobin and cytochrome and to catalyze the reduction of the $NAD^+$ [31]. PLH modified sensors and biosensors are used to determine various analytes [32, 33]. Several methods for polymerizing L-histidine on the electrode surface have been previously reported [5, 32, 33].

In this study, an amperometric biosensor has been fabricated by immobilizing HRP on PLH, multiwall carbon nanotube, and IL modified glassy carbon electrode (HRP/PLH/MWCNT-IL/GCE) for the sensitive quantification of $H_2O_2$. HRP was electrostatically immobilized on the PLH/MWCNT-IL/GCE. Following the optimization of the experimental conditions the analytical performance characteristics of the HRP/PLH/MWCNT-IL/GCE have been determined. The analytical application of the biosensor for the $H_2O_2$ determination in real samples was also studied.

## Results and discussion

### Optimization of HRP/PLH/MWCNT-IL/GCE composition

In order to improve the efficiency of HRP/PLH/MWCNT-IL/GCE, certain amounts of MWCNT, IL, and HRP used in the electrode composition were optimized. For this, the amount of the optimization material varied, whereas the amount of the other components was kept constant. In the optimization of the amount of MWCNT and IL, the level of HRP on the surface of the electrode was kept constant at 20.4 U.

The effects of the IL amount on the response of the HRP/PLH/MWCNT-IL/GCE were investigated by varying its amount in the MWCNT-IL-gelatin mixture as 2.5, 5.0, 7.5, and 10.0 $mm^3$. The amount of MWCNT is of 1.5 mg $cm^{-3}$. Figure 1A shows the $H_2O_2$ responses to HRP/PLH/MWCNT-IL/GCEs as fabricated with the studied IL amounts. As the amount of IL increased from 2.5 $mm^3$ to 7.5 $mm^3$, the current response improved and then decreased. The biosensor showed the best current response to be at 7.5 $mm^3$ IL and this value was used as the optimal amount of IL for the fabrication of the modified electrode.

MWCNT-IL-gelatin mixture containing different amounts of MWCNT (1.0, 1.5, 2.0, and 2.5 mg $cm^{-3}$) was investigated for its effect on the amperometric $H_2O_2$ response by four different HRP/PLH/MWCNT-IL/GCE. As shown in Fig. 1B, the sensitivity of the fabricated $H_2O_2$ biosensor increased with the amount of MWCNT up to 2.0 mg $cm^{-3}$ and decreased afterwards. At high MWCNT amounts, the thickening of the electrode surface caused the shedding of

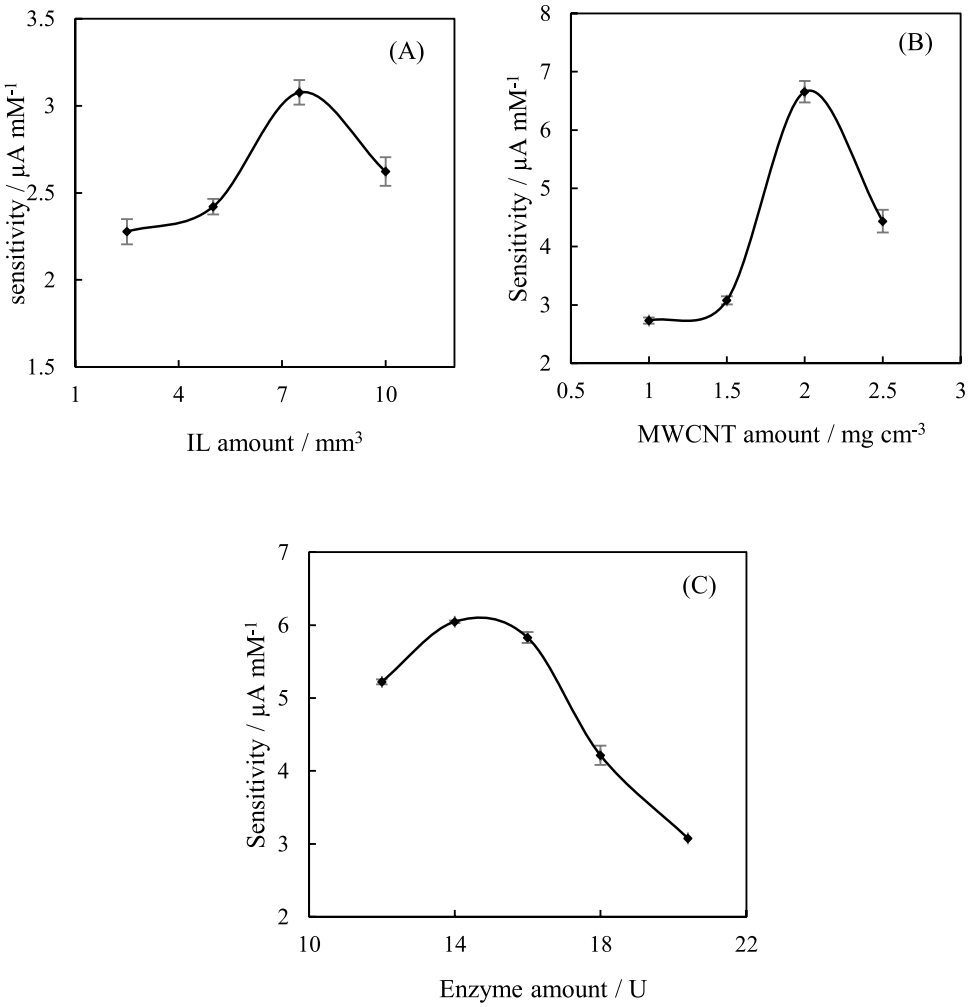


**Fig. 1** Effects of **A** IL, **B** MWCNT, **C** HRP amounts on the response of HRP/PLH/MWCNT-IL/GCE (in 0.05 M pH 7.0 PBS, $E_{app} = -0.1$ V)

the modified material over time. This is the reason why current responses with low repeatability were recorded. Consequently, the optimum amount of MWCNT was selected to be of 1.5 mg $cm^{-3}$.

The effect of HRP amount on HRP/PLH/MWCNT-IL/GCE biosensor response was also investigated. The $H_2O_2$ sensitivity of the fabricated biosensors at different enzyme units is shown in Fig. 1C. The sensitivity increased with the HRP up to 13.9 U and decreased afterwards. The decreased biosensor response at higher HRP units is hypothesized to be the result of an increased electron transfer resistance [34]. Consequently, 13.9 U HRP was selected as the optimal amount.

## Determination of the surface morphology of modified biosensor

SEM and EDX techniques were used to evaluate the surface morphology of the modified $H_2O_2$ biosensor. The SEM images of MWCNT/SPE, MWCNT-IL/SPE, PLH/MWCNT-IL/SPE, and HRP/PLH/MWCNT-IL/SPE are given in Figs. 2A-a and A-b, respectively. The SEM image of MWCNT-IL/SPE clearly shows the homogeneous distribution of the MWCNT-IL composite (Fig. 2A-b). A more porous morphology was observed with the addition of IL to MWCNT/SPE. Distinct plates and rods which were observed on the PLH/MWCNT- IL/SPE surface (Fig. 2A-c) indicate the well-coated PLH on the electrode surface [5]. The transformation of the rod and plate structures on the PLH/MWCNT-IL/SPE surface into a more ordered form confirms the immobilization of HRP on the electrode surface (Fig. 2A-d). The electrostatic immobilization of the negatively charged HRP on the positively charged PLH/MWCNT-IL/SPE surface can be explained by different surface morphology. The EDX spectrum of HRP/PLH/MWCNT-IL/SPE is also given in Fig. 2B. The C, O, and N peaks in the spectrum can be attributed to histidine on the electrode surface. The P and F peaks in the spectrum are due to the existence of IL.

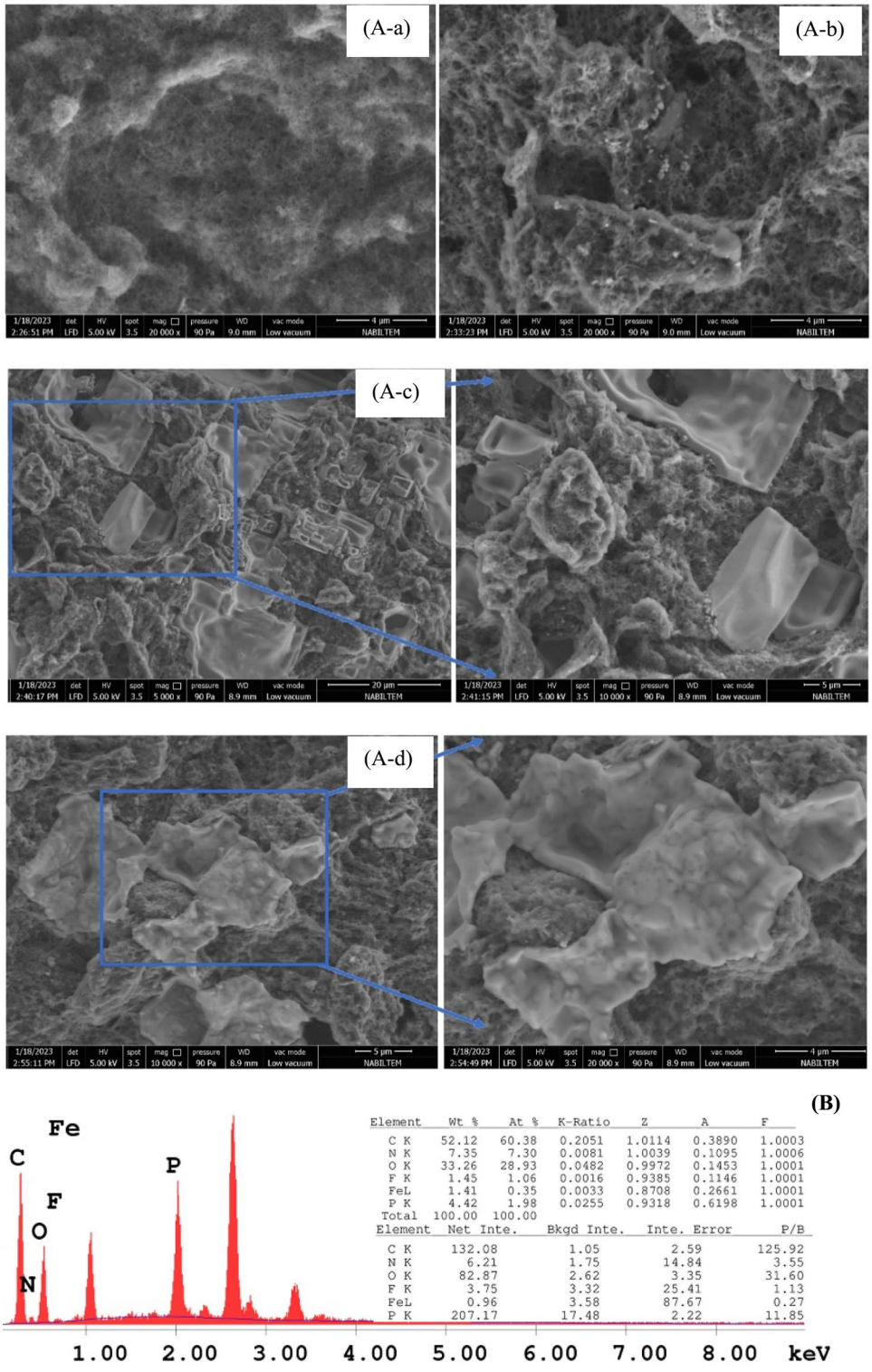


**Fig. 2** **A** SEM images of (**a**) MWCNT/SPE, (**b**) MWCNT-IL/SPE, (**c**) PLH/MWCNT-IL/SPE, (**d**) HRP/PLH/MWCNT-IL/SPE; **B** EDX spectra of HRP/PLH/MWCNT-IL/SPE

## Electrochemical properties of HRP/PLH/MWCNT-IL/GCE

The electrochemical properties of the electrode surface occurring after each modification step were investigated by CV and EIS methods. For this purpose, cyclic voltammograms and EIS of bare GCE, MWCNT-IL/GCE, PLH/MWCNT-IL/GCE, and HRP/PLH/MWCNT-IL/GCE were recorded in 5.0 mM $K_3Fe(CN)_6/K_4Fe(CN)_6$ (1:1) solution containing 0.1 M KCl (Fig. 3).

Cyclic voltammetry measurements are effective tools to elucidate the electrochemical properties of the modified

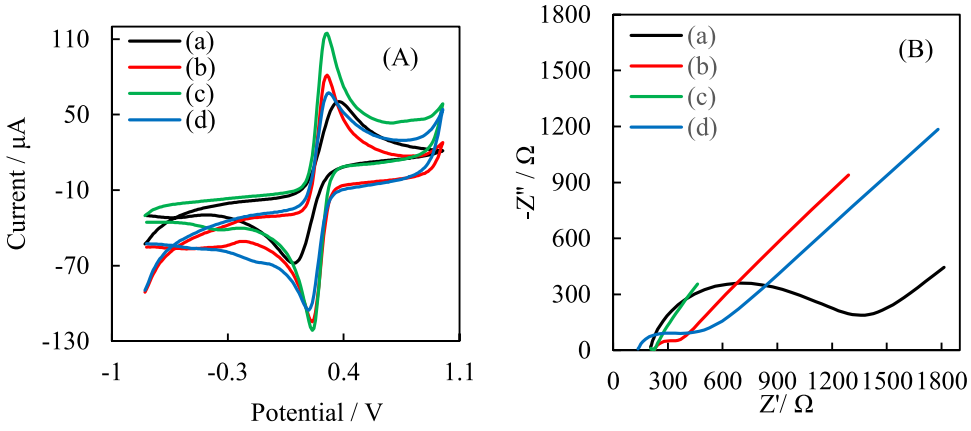


**Fig. 3** **A** Cyclic voltammogram (scan rate: 0.05 V $s^{-1}$), **B** Nyquist plots (**a**) bare GCE, (**b**) MWCNT-IL/GCE, (**c**) PLH/MWCNT-IL/GCE, (**d**) HRP/PLH/MWCNT-IL/GCE in 5 mM $[Fe(CN)_6]^{3-/4-}$ solution containing 0.1 M KCl

electrodes after each modification step. In CV measurements, well-defined redox peaks at + 0.420 V and + 0.090 V were observed at bare GCE (Fig. 3A-a). There is a difference of 0.330 V between the anodic and cathodic peak potentials of $[Fe(CN)_6]^{3-/4-}$ at bare GCE. Figure 3A-b shows that the peak currents are more intense in MWCNT-IL/GCE than at bare GCE. There is also a difference of 0.090 V between the peak potentials of the redox probe. This result can be attributed to the larger surface area of the MWCNT-IL composite as compared to the GCE electrode surface and the enhanced electron transfer between the redox probe and the electrode [12, 19, 35]. In the voltammogram obtained at PLH/MWCNT-IL/GCE, the current intensity of the redox peaks increased while the peak separation remained the same (Fig. 3A-c). This result can be attributed to the attraction between the positively charged electrode surface and the negatively charged redox probe due to intense electrostatic interaction [5]. Immobilization of HRP enzyme on the electrode surface decreased significantly the redox peak currents, where the difference between the peak potentials was of 0.120 V (Fig. 3A-d). The decrease in the peak currents and the increase in the peak potential difference can be explained by the thickened electrode surface, the barrier effect of Nafion, and the repulsion between the negatively charged HRP and the redox probe. This result constitutes the evidence for the successful immobilization of the HRP on the surface of the electrode.

EIS measurements were carried out in order to investigate more thoroughly the electrochemical properties of the modified electrodes. In EIS measurements, the $R_{ct}$ value of bare GCE was determined as 1089 Ω (Fig. 3B-a). After GCE was modified with MWCNT-IL composite, the $R_{ct}$ value decreased to 109.5 Ω (Fig. 3B-b). When the MWCNT-IL/GCE surface was coated with PLH, this value was determined as 17.01 Ω (Fig. 3B-c). The reason for the significant decrease in $R_{ct}$ value is the strong electrostatic interaction between the positive amino groups in PLH and the negatively charged redox probe. The immobilization of HRP on the PLH/MWCNT-IL/GCE surface increased the $R_{ct}$ value to 374.9 Ω (Fig. 3B-d). This increase can be attributed to the repulsion between the negatively charged HRP and the redox probe. This result is a consequence of the successful immobilization of HRP on PLH/MWCNT-IL/GCE.

## Optimizing experimental conditions

The operating potential and pH have been optimized to improve the performance of the $H_2O_2$ biosensor. For this purpose, the effects of pH on HRP/PLH/MWCNT-IL/GCE performance were tested at pH values between 5.0 and 8.0. Figure 4A shows that the $H_2O_2$ sensitivity of HRP/PLH/MWCNT-IL/GCE increases from pH 5.0 to 6.5 and decreases from pH 6.5 to 8.0. The optimum pH was found to be of pH 6.5 with the highest current response.

The operating potential values were changed between −0.15 V and 0.0 V to determine the optimum potential (Fig. 4B). As the applied potential changed from −0.15 V to −0.1 V, the response of the biosensor increased and decreased at more positive potential values. The highest sensitivity was obtained at −0.1 V and this working potential was selected as the optimum potential.

## Analytical characterization of biosensor

The response of HRP/PLH/MWCNT-IL/GCE to $H_2O_2$ was investigated after optimizing the experimental conditions. The amperometric response of HRP/PLH/MWCNT-IL/GCE was measured by successive addition of $H_2O_2$ in 0.05 M pH 6.5 PBS at −0.1 V. Figure 5A shows that a stable, rapid, and well-defined amperometric response is observed after each addition of $H_2O_2$. This indicates the efficacy of HRP/PLH/MWCNT-IL/GCE for the biorecognition event. The corresponding calibration curve plotted from the i-t data is shown in Fig. 5B. The response of HRP/PLH/MWCNT-IL/GCE to $H_2O_2$ showed two different linear operating ranges from $2.0 \times 10^{-2}$ µM to $9.1 \times 10^{-1}$ µM

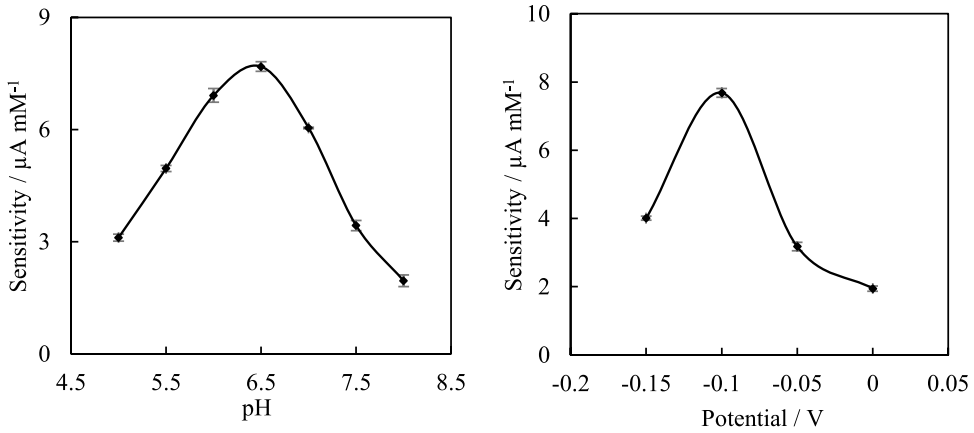


**Fig. 4** The effects of **A** buffer pH (in 0.05 M PBS, $E_{app} = -0.1$ V) and **B** applied potential (0.05 M pH 6.5 PBS) on the response of HRP/PLH/MWCNT-IL/GCE

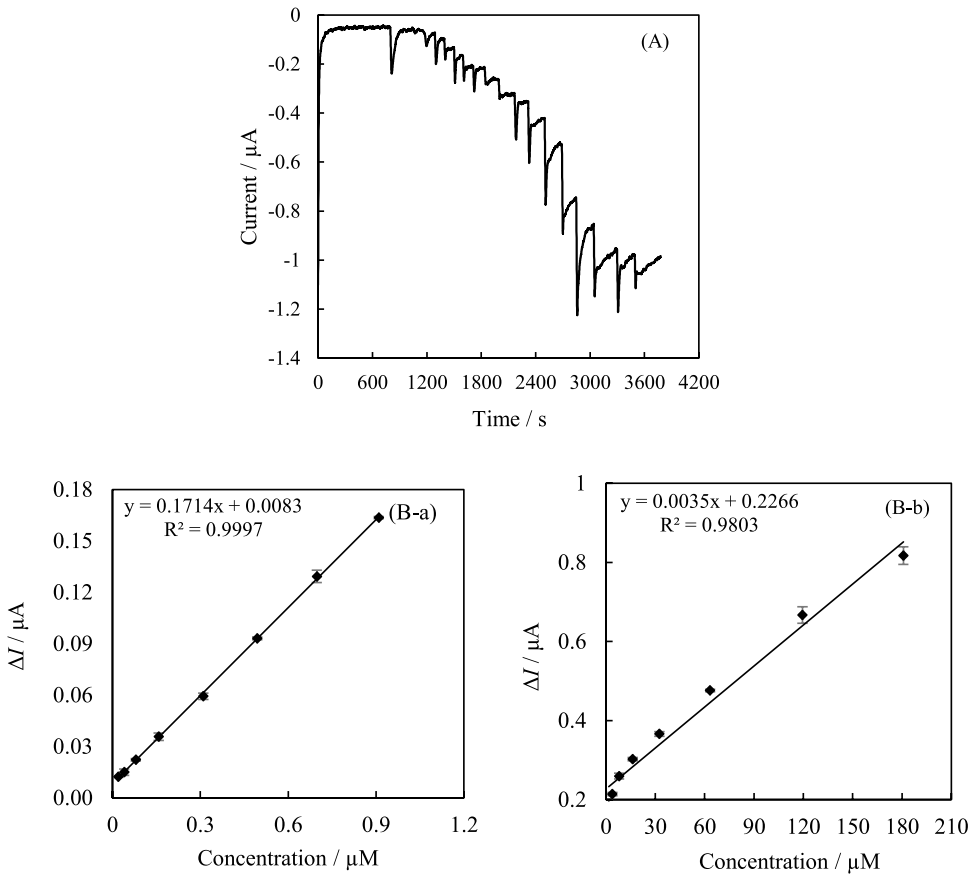


**Fig. 5** **A** Current–time response of HRP/PLH/MWCNT-IL/GCE to the successive additions of $H_2O_2$ and **B** calibration curves of the HRP/PLH/MWCNT-IL/GCE (**a**) first linear range (**b**) second linear range (in 0.05 M pH 6.5 PBS, $E_{app} = -0.1$ V)

and from 1.8 μM to 180 μM. The limit of detection (LOD) and the limit of quantitation (LOQ) of HRP/PLH/MWCNT-IL/GCE were calculated as $2.9 \times 10^{-3}$ μM and $9.5 \times 10^{-3}$ μM from Eqs. 3 *sb/m* and 10 *sb/m*, respectively. In the given equation, *m* is the slope of the calibration curve, *sb* is the standard deviation of the current differences obtained by different measurements ($n = 10$) of $H_2O_2$ solution at constant concentration ($2.0 \times 10^{-2}$ μM). HRP/PLH/MWCNT-IL/GCE reached 95% of the steady-state current in approximatively 15 s.

The reproducibility of the proposed biosensor was assessed by plotting the $H_2O_2$ calibration curves of five HRP/PLH/MWCNT-IL/GCEs fabricated through the same process. The slope of the calibration curve was used to calculate the reproducibility of the HRP/PLH/MWCNT-IL/GCE in terms of relative standard deviation (RSD) and it was found to be of 0.71%. This result shows that the presented (bio)sensor has a very good reproducibility.

The response of HRP/PLH/MWCNT-IL/GCE to 0.16 μM $H_2O_2$ solution was recorded for ten times in order to prove

its working stability. After these 10 measurements, only a 2.52% loss in activity was observed, which confirms the good operating stability of the $H_2O_2$ biosensor. The long-term stability of HRP/PLH/MWCNT-IL/GCE was investigated. The $H_2O_2$ response of the biosensor was recorded for three weeks. Modified GCEs were stored at + 4 °C during the experiments. HRP/PLH/MWCNT-IL/GCE showed 93.6%, 82.5%, and 80.1% of the amperometric response at the end of days 5, 10, and 21, respectively. Based on this result, it can be confirmed that the biosensor possesses a good long-term stability. The performance parameters of the HRP/PLH/MWCNT-IL/GCE biosensor is given in Table 1.

The selectivity of the HRP/PLH/MWCNT-IL/GCE biosensor was investigated in the presence of some possible interferents, such as sodium chloride, glutamic acid, oxalic acid, and glucose. Amperometric measurements of the HRP/PLH/MWCNT-IL/GCE biosensor to successive additions of 0.09 mM $H_2O_2$ and 0.09 mM of each interfering substance to a stirred 0.05 M PBS solution were recorded. The results indicated that sodium chloride, glutamic acid, oxalic acid, and glucose provide 3.2%, 0.4%, 0.2%, and 1.7% interference on the $H_2O_2$ response of HRP/PLH/MWCNT-IL/GCE, respectively. The low operating potential and the blocking role of Nafion are responsible for the good selectivity.

### Determination of $H_2O_2$ in oxygenated water

The amount of $H_2O_2$ in commercial disinfectant samples was determined by the standard addition method to verify the potential applications of HRP/PLH/MWCNT-IL/GCE. Table 2 shows the amounts of $H_2O_2$ in the disinfectant sample determined by the developed (bio)sensor. The recoveries were found to be between 97.2% and 101.7%. These results show that the fabricated $H_2O_2$ biosensor is accurate and precise to an acceptable level.

Table 3 compares the analytical performance of the $H_2O_2$ biosensor fabricated by us with some other biosensors documented in the literature. In the table, it can be seen that HRP/PLH/MWCNT-IL/GCE offers high sensitivity, wide operating range, and low detection limit as compared to most of the previous $H_2O_2$ biosensors. This improved efficiency is due to the strong immobilization of PLH and HRP, the synergistic effects of the modifying substrates, and the low working potential.

## Conclusion

The present study proves that the modified electrode surface fabricated by electrochemical polymerization of L-histidine on MWCNT-IL composite provides a suitable environment for electrostatic immobilization of HRP. In order to develop a biosensor with high sensitivity and accuracy, the amount of MWCNT, IL, and enzyme was optimized and suitable operating conditions were determined. The designed biosensor shows wide operating range, high sensitivity, low detection limit, good stability, and good storage stability. These results indicate that the limited biosensor application involving electrostatic immobilization of HRP should be more widely used in the future.

## Experimental

HRP (from horseradish type VI with a specific activity of 273 units/mg solid), hydrogen peroxide, sodium monohydrogen phosphate, sodium dihydrogen phosphate, sodium hydroxide, hydrochloric acid, 1-butyl-3-methylimidazolium tetrafluorophosphate, potassium hexacyanoferrate(III), potassium hexacyanoferrate(II), Nafion (5% by weight in lower aliphatic alcohols), oxalic acid, bovine skin gelatin (type B), and L-histidine were purchased from Sigma-Aldrich and used as provided. Potassium chloride, glutamic acid, and sodium chloride were obtained from Merck, and

**Table 1** The analytical performance parameters of the developed biosensor

| Performance parameters | HRP/PLH/MWCNT-IL/GCE |
|---|---|
| First linear working range/μM | $2.0\times10^{-2}$–$9.1\times10^{-1}$ |
| Second linear working range/μM | 1.8–180 |
| LOD/μM | $2.9\times10^{-3}$ |
| Sensitivity/μA $\mu M^{-1}$ | 0.1714<br>0.0035 |
| Reproducibility/% | 0.71 |
| Operational stability/% | 2.52 |
| Long term stability | 20% loss after 21 days |

**Table 2** $H_2O_2$ determination in oxygenated water sample

| Sample | Added $H_2O_2$/μg $dm^{-3}$ | Found $H_2O_2$/μg $dm^{-3}$ | Recovery/% |
|---|---|---|---|
| Oxygenated water (10 $mm^3$) | 2.99 | 3.0; 2.97; 3.04 | 100.5; 99.2; 101.7 |
| | | 3.0 ± 0.04 | 100.5 ± 1.3 |
| Oxygenated water (20 $mm^3$) | 6.12 | 5.95; 6.09; 6.05 | 97.2; 97.4; 98.9 |
| | | 6.03 ± 0.07 | 98.5 ± 1.2 |

**Table 3** Comparison of the analytical performance parameters of different amperometric $H_2O_2$ biosensors earlier reported in the literature

| Modified electrodes | Linear range/μM | LOD/μM | Samples | Recovery/% | References |
|---|---|---|---|---|---|
| HRP/PLH/MWCNT-IL/GCE | 0.02–0.9<br>1.8–180 | 0.0029 | Oxygenated water | 97.2–101.7 | This study |
| HRP/P-L-His-RGO/GCE | 0.2–5000 | 0.05 | Real eye drop | 98.0–101.0 | [5] |
| Au–Pd/rGO/GCE | 0.005–3500 | 0.004 | Human serum | 97.0–103.0 | [36] |
| HRP-AuNCs/MWCNTs/CFUMEs | 2.0–24 | 0.443 | Calf serum sample | 93.6 | [37] |
| GCE/P(GMA-co-VFc) | 2000–30,000 | 2.6 | $H_2O_2$ samples | 94.4–101.1 | [38] |
| b-HRP/MWCNTs-avidin/GCE | 1.0–14 | 0.024 | Mouthwash | 95.3 | [39] |
| | | | Human blood serum | 105.2 | |
| | | | Milk | 90.8 | |
| $NiCo_2S_4$/rGO/GCE | 25–11,250 | 0.19 | Milk | 97.1 | [40] |
| | | | Toner | 100.4 | |
| $NH_2$-MIL-53(Fe)/HRP/MWCNTs/GCE | 0.1–1.0 | 0.028 | Hela cell culture | 120.4 | [41] |
| | 1.0–600 | | HepG2 cell culture | 113.0 | |
| HEPNP/rGO/Au electrode | 0.01–100 | 0.01 | Human serum sample | – | [42] |
| Mn(II)-PLH-CMWCNT/GCE | 2.0–1000 | 0.5 | Diluted disinfectant fetal bovine serum | 96.5–105<br>96–103.5 | [43] |

*P-L-His and PLH* poly-L-histidine, *rGO* reduced graphene oxide, *AuNCs* functionalized fluorescent gold nanoclusters, *CFUMEs* coated carbon fiber ultramicroelectrodes, *P(GMA-co-VFc)* poly(glycidyl methacrylate-co-vinyl ferrocene), *$NiCo_2S_4$* bimetallic nickel cobalt sulfides, *$NH_2$-MIL-53(Fe)* hybrid of metal organic framework, *HEPNP* horseradish peroxidase encapsulated protein nanoparticles, *Mn(II)-PLH-CMWCNT* manganese(II)-poly-L-histidine functionalized carboxylated multi-walled carbon nanotubes, *HRP* horseradish peroxidase, *MWCNTs* Multiwall carbon nanotubes

glucose was obtained from Fluka. MWCNTs (O.D. < 8 nm; length 10–30 μm) were obtained from Cheap Tubes Inc. (Brattleboro, USA). Double distilled water was used for all experiments. Commercial oxygenated water samples for the sampling practices were obtained from a local pharmacy in the city of Tekirdağ, Türkiye.

Electrochemical measurements and electrochemical impedance measurements (EIS) were performed by Microstat 400 (Dropsens, Spain) and Gamry Instrument (Reference 300) bipotentiostat/galvanostat instruments, respectively. A three-electrode cell system consisting of a modified GCE (BASi MF 2012, diameter 3 mm) as working electrode, a platinum wire (BASi MW1032, Bioanalytical Systems, Inc., USA) as auxiliary electrode and an Ag/AgCl electrode (BASi MF 2052) as reference electrode were also used. SEM and EDX studies were performed using a Field Emission Scanning Electron Microscope (FE-SEM, QUANTA FEG-250). SPCE (Dropsens C110), containing a carbon working electrode, a silver pseudo reference electrode, and a carbon counter electrode, was used to perform the SEM and EDX measurements.

## Electrochemical measurements

In the optimization studies, the amperometric response of the biosensor to $H_2O_2$ concentrations between 0.03 mM and 0.2 mM (0.03, 0.05, 0.07, 0.09, 0.1, and 0.2 mM) was measured, and their sensitivities (slopes of the calibration graphs) were compared. CV and EIS studies were performed in 5.0 mM $K_3Fe(CN)_6/K_4Fe(CN)_6$ (1:1) with 0.1 M KCl from − 0.8 V to + 1.0 V at a scan rate of 50 mV $s^{-1}$. The figures are shown with error bars. The error bars represent the standard deviation of the three measurements.

## Fabrication of HRP/PLH/MWCNT-IL/GCE

The GCE surface was treated with $Al_2O_3$ paste (0.05 μm) for 10 min. Then the GCE surface was sonicated with distilled water and ethanol-pure water (1:1) mixture for 5 min in an ultrasonic bath. 1 mg of gelatin was suspended in 1 $cm^3$ distilled water and kept on a magnetic stirrer at 35 °C−40 °C for 10 min. A mixture of 1.5 mg MWCNT and 7.5 $mm^3$ IL was added to 1.0 $cm^3$ of gelatin solution and dispersed homogeneously in an ultrasonic bath for 1 h. 5 $mm^3$ of MWCNT-IL-gelatin mixture was dropped onto GCE. The mixture was allowed to dry at room temperature. Cyclic voltammograms of MWCNT-IL/GCE versus Ag/AgCl in solution containing 5 mM L-His (0.05 M pH = 5.0 PBS) were recorded at 50 mV $s^{-1}$ with 30 cycles in the potential range of 0.0 to – (− 1.5 V). PLH/MWCNT-IL/GCE was cleaned with distilled water and allowed to dry at room temperature. 2.93 mg of HRP were added to 200 $mm^3$ of 0.05 M PBS (pH 7). 3.5 $mm^3$ of the enzyme dilution (4 U/$mm^3$) was pipetted onto PLH/MWCNT-IL/GCE. Finally, 5.0 $mm^3$ 0.1% Nafion was added. The HRP/PLH/MWCNT-IL/GCE was stored at + 4 °C overnight (Fig. 6).

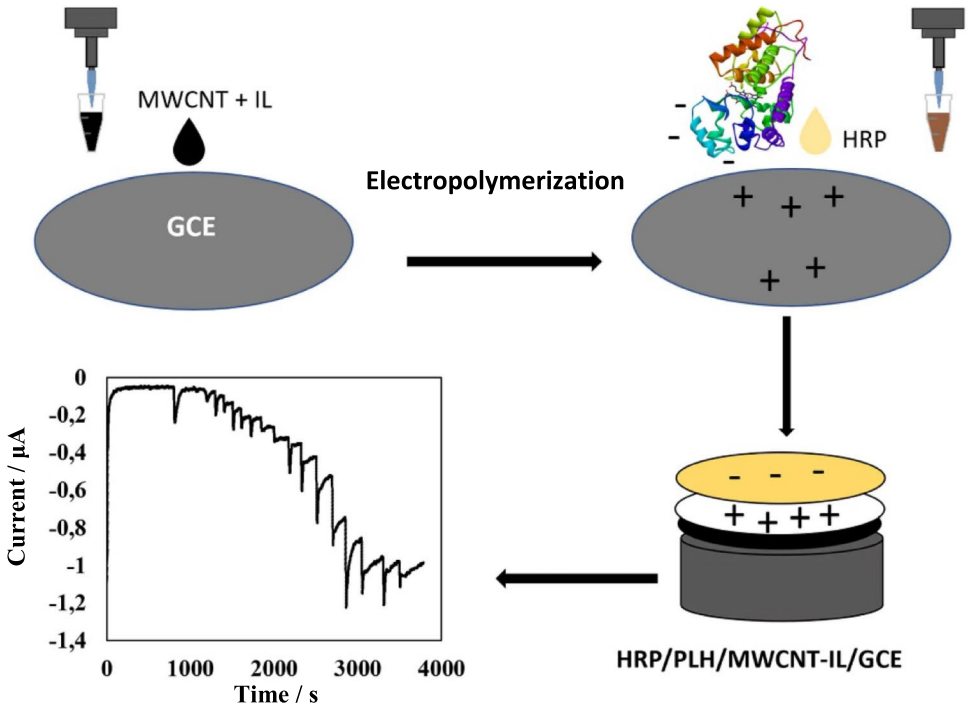


**Fig. 6** Fabrication of HRP/PLH/MWCNT-IL/GCE

**Acknowledgements** This study was supported by Tekirdağ Namık Kemal University Scientific Research Projects Coordination Unit (Project No: NKUBAP.01.GA.19.202).

**Data availability** The data that support the findings of this study are available from the corresponding author upon reasonable request.

## References

1. Xing L, Zhang W, Fu L, Lorenzo JM, Hao Y (2022) Food Chem 385:132555
2. Rashed Md-A, Ahmed J, Faisal M, Alsareii SA, Jalalah M, Tirth V, Harraz FA (2022) Surf Interfaces 31:101998
3. Pramanik D, Dey SG (2011) J Am Chem Soc 133:81
4. Wei Y, Zhang Y, Liu Z, Guo M (2010) Chem Commun 46:4472
5. Vilian ATE, Chen SM (2014) RSC Adv 4:55867
6. King DW, Cooper WJ, Rusak SA, Peake BM, Kiddle JJ, O'Sullivan DW, Melamed ML, Morgan CR, Theberge SM (2007) Anal Chem 79:4169
7. Baga AN, Alastaır Johnson GR, Nazhat NB, Saadalla-Nazhat RA (1988) Anal Chim Acta 204:349
8. Mccurdy WH Jr, Bell HF (1966) Talanta 13:925
9. Gupta V, Mahbub P, Nesterenko PN, Paull B (2018) Anal Chim Acta 1005:81
10. Mihailova I, Gerbreders V, Krasovska M, Sledevskis E, Mizers V, Bulanovs A, Ogurcovs A (2022) Beilstein J Nanotechnol 13:424
11. Ensafi AA, Abarghoui MM, Rezaei B (2014) Sens Actuators B 196:398
12. Tunca K, Öztürk F, Erden PE (2022) Electroanal 34:1092
13. Tang J, Wang B, Wu Z, Han X, Dong S, Wang E (2003) Biosens Bioelectron 18:867
14. Li J, Tan SN, Ge H (1996) Anal Chim Acta 335:137
15. Zhang W, Guo C, Chang Y, Wu Fengyan, Ding S (2014) Monatsh Chem 145:107
16. Li X, Wang L, Wang B, Zhang S, Jiang M, Fu W, Sun W (2022) Molecules 27:8064
17. Settu K, Lai YC, Liao CT (2021) Mater Lett 300:130106
18. Saeed AA, Abbas MN, El-Hawary WF, Issa YM, Singh B (2022) Biosensors 12:778
19. Wan J, Bi J, Du P, Zhang S (2009) Anal Biochem 386:256
20. Haghighi B, Hamidi H, Gorton L (2010) Electrochim Acta 55:4750
21. Murphy M, Theyagarajan K, Prabusankar G, Senthilkumar S, Thenmozhi K (2019) Appl Surf Sci 492:718
22. Liu X, Bu C, Nan Z, Zheng L, Qiu Y, Lu X (2013) Talanta 105:63
23. Huang BQ, Wang L, Shi K, Xie ZX, Zheng LS (2008) J Electroanal Chem 615:19
24. Wang L, Feng Z, Cai H (2009) J Electroanal Chem 636:36
25. Baksh H, Buledi JA, Khand NH, Solangi AR, Mallah A, Sherazi ST, Abro MI (2020) Monatsh Chem 151:1689
26. Haghighi B, Khosravi M, Barati A (2014) Mater Sci Eng 40:204
27. Canbay E, Türkmen H, Akyılmaz E (2014) Bull Mater Sci 37:617
28. Ji H, Zhu L, Liang D, Liu Y, Cai L, Zhang S, Liu S (2009) Electrochim Acta 54:7429
29. Chattopadhyay K, Mazumdar S (2000) Biochemistry 39:263
30. Dıaz AN, Peinado MCR, Minguez MCT (1998) Anal Chim Acta 363:221
31. Bergamini MF, Santos DP, Zanoni MVB (2009) J Braz Chem Soc 20:100
32. Bergamini MF, Santos DP, Zanoni MVB (2010) Bioelectrochem 77:133
33. Bergamini MF, Santos DP, Zanoni MVB (2013) J Electroanal Chem 690:47
34. Campuzano S, Serra B, Pedrero M, Villena FJM, Pingarron JM (2003) Electroanal 494:187
35. Xiao L, Ding Y, Zhai Q, Hu M, Li S, Wang Y, Chen Y, Jiang Y (2019) J Electrochem Soc 166:G67
36. Dong W, Ren Y, Bai Z, Yang Y, Chen Q (2019) Bioelectrochem 128:274
37. Ren QQ, Yang F, Ren W, Wang C, Jiang WS, Zhao Z, Chen J, Lu XY, Yu Y (2020) Hindawi J Nanomater 9627697

38. Şenel M, Cevika E, Abasıyanık MF (2010) Sens Actuators B 145:444
39. Gutierrez FA, Rubianes MD, Rivas GA (2019) Anal Chim Acta 1065:12
40. Wang M, Ma J, Guan X, Peng W, Fan X, Zhang G, Zhang F, Li Y (2019) J Alloys Compd 784:827
41. Jiang T, Sun X, Wei L, Li M (2020) Anal Chim Acta 1135:132
42. Shin JH, Lee MJ, Choi JH, Song J, Kim TH, Oh BK (2020) Nano Convergence 7:1
43. Zhou J, Chen Y, Lan L, Zhang C, Pan M, Wang Y, Han B, Wang Z, Jiao J, Chen Q (2019) Anal Biochem 567:51